High Responsivity and Detectivity Graphene-Silicon Majority Carrier Tunneling Photodiodes with a Thin Native Oxide Layer

*Hong-Ki Park and Jaewu Choi**

Quantum Information Display Laboratory, Department of Information Display, Kyung Hee University, 26, Kyungheedae-ro, Dongdaemun-gu, Seoul, 02447, Republic of Korea.

Corresponding Authors:

*E-mail (Jaewu Choi): jaewuchoi@khu.ac.kr

Supporting information

Table of contents

1. The Mott-Schottky plot

Figure S1 shows the Mott-Schottky plot of the experimental C-V measurement taken from the GOS device at 1kHz.[1,2] The built-in potential (V_{Bi}) is estimated as ~ 0.1 V indicated by the extrapolated linear curves ($1/C^2$ vs V) to x-axis. Using the relationship of $\frac{1}{C^2} = \frac{2}{qAN_A\varepsilon_0\varepsilon_{SiO_2}}[V - V_D]$, where N_A is the acceptor concentration, ε_0 is the vacuum permittivity and ε_{SiO_2} is the relative permittivity of SiO_2, the Si doping concentration, $N_A = \frac{2}{\varepsilon_0\varepsilon_{SiO_2}q}\left[\frac{d(1/C^2)}{dV}\right]^{-1}$, is estimated as ~ 1.32 x 10^{15} cm^{-3}. The relationship of $E_{F(Si)} = E_{i(Si)} + kTln(N_A/n_i)$ says that the corresponding Fermi level of the employed Si ($E_{F(Si)}$) is~ 4.86 eV where $E_{i(Si)}$ is the intrinsic level of the bulk Si (assumed to be 4.61 eV) and n_i is the intrinsic carrier concentration at room temperature (assumed to be 1.5 x 10^{10} cm^{-3}).

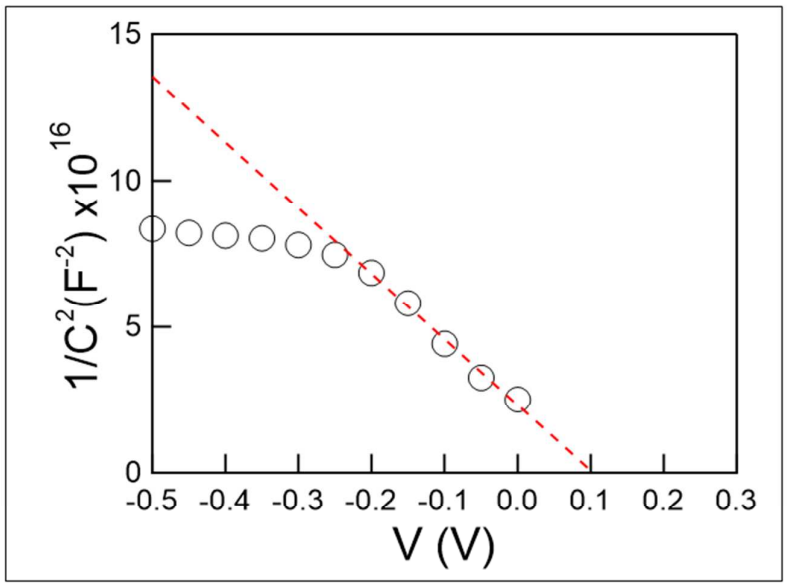

Figure S1. Mott-Schottky plot of the C-V curve taken from a GOS diode at 1 kHz AC modulation at dark state.

2. Voltage and optical power dependent Raman spectra of graphene

Raman spectra were measured from the middle of GOS structures using a 515 nm wavelength

Ar-ion laser and a 100x microscope objective lens. The beam spot size employed for Raman studies is about 1 μm in diameter. The employed laser power was varied from 0.024 mW to 1 mW.[3] Raman spectra were taken at zero bias voltage as well as -5 V reverse bias voltage.

Figure S2a shows the optical power-dependent Raman shift of the GOS junction at the reverse bias voltages of -5 V as well as at zero bias voltage (0 V). The peak position of the G band is varied with the reverse bias voltage as well as the optical power as shown in the inset of Figure S2b. This suggests that the graphene Fermi level depends on the reverse bias voltage as well as the optical power.

The estimated graphene Fermi level or the charge carrier concentration from the G peak position are plotted in Figure S2b while the graphene Fermi level ($E_{F(G)}(p)$) is related to the hole concentration (p) in graphene as $E_{F(G)}(p) = \hbar|v_F|\sqrt{\pi p}$, where $\hbar$ is the reduced Planck constant and v_F is the Fermi velocity (10^6 ms^{-1}) in graphene.[4-6]

At the low laser optical power of 0.024 mW, the G peak positions at zero bias voltage (○) located at ~1585.6 cm^{-1} (ΔE_F = 0.186 eV) is shifted to ~ 1585.8 cm^{-1} (ΔE_F = 0.196 eV) at the reverse bias voltage of -5 V (□). As a result, the carrier density (p) in graphene at the reverse bias voltage of -5 V increases by more than 10 % of that at 0 V as shown in Figure S2b. The bias voltage dependent graphene Fermi level shift of the employed GOS devices is relatively low compared to that observed from a similar structure.[1] This is attributed that the thin native oxide thickness of the present GOS (4.2 Å) is less than that (5.3 Å) reported previously.[1] The higher tunneling rate due to the thinner oxide layer causes lower charge accumulation across the native oxide layer and thus lower the graphene Fermi level shift.

With the initial increase of the optical power, the G peak position (~1586.3 cm^{-1}), the carrier density (3.19 x 10^{12} cm^{-2}) and the Fermi level (ΔE_F = 0.209 eV) slightly shift to higher values as shown in Figure S2b. However, the further increase of the laser power, the G peak position, the density and the Fermi level shift become even lower than that at 0 V as shown in Figure S2b.[3] At the initial exposure of the low optical power, photo-generated electrons are accumulated at the native oxide/Si interface while the graphene layer is charging with holes. As a result, the graphene becomes more p-

doped. However, when the optical power becomes higher than a critical optical power, the enhanced photo-induced carrier tunneling caused by the Schottky barrier lowering reduces the hole concentration in graphene as the optical power increases. In addition to this, the minority carriers tunneled from the silicon are recombined with the holes in graphene. However, further increase of the probe laser optical power, the graphene Fermi level is insensitive to the optical power. In addition to the higher tunneling rate, this is attributed to the density of state in graphene, which is proportional to the energy from the Dirac point.

However, the employed optical power density for the optical response study of the GOS devices are far less than the optical power density employed for the Raman study. Thus, this study suggests that the Fermi level shift of the graphene in the GOS structures by the employed LED optical power density can be negligible compared to the oxide voltage appeared across the native oxide layer while the graphene Fermi level shift by the reverse bias voltage is tangible as shown in Figure S2.

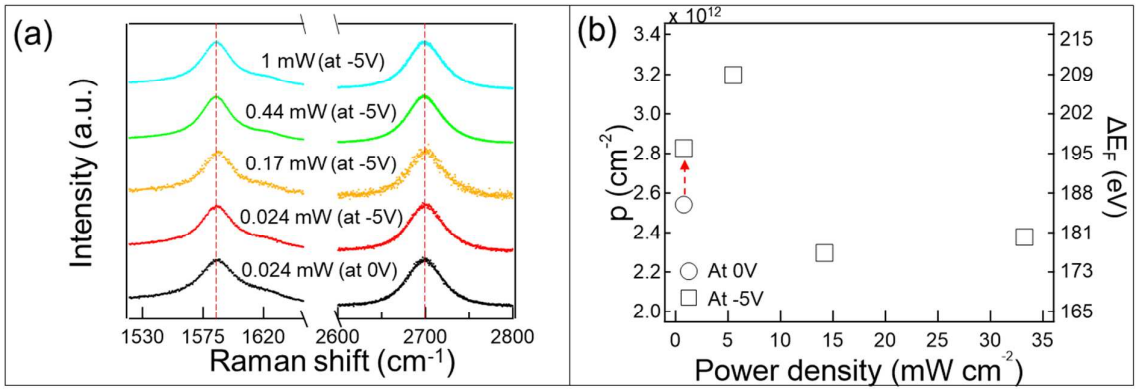

Figure S2. (a) Raman spectra of the GOS diode taken by a laser power of 0.024 mW at 0V, and as a function of laser power (0.024 mW ~ 1 mW) at the bias voltage of –5V. (b) Hole doping concentration (p) and graphene Fermi level position, $\Delta E_{F(G)}(p) = \hbar|v_F|\sqrt{\pi p}$, at -5 V reverse bias voltage as a function of laser power and marked by squares (□). Those at 0 V are marked by circles (○).

3. Optical power dependent C-V curves and their fitting results

For the analysis of the photo-capacitance in GOS Schottky diodes, an equivalent circuit model is

composed of capacitance network as shown in Figure S3a. The GOS Schottky diode is modeled as a capacitance network of aluminum-graphene contact (Al-G), graphene (G), silicon diode (SiO_2), depletion region (D), the interface state (int), inversion region (inv) and gold-silicon contact capacitances. Based on the equivalent circuit model in Figure S3a, the total capacitance (C) is given by

$$\frac{1}{C} = \frac{1}{C_{Al-G}} + \frac{1}{C_G} + \frac{1}{C_{SiO2}} + \frac{1}{C_D + C_{int} + C_{inv}} + \frac{1}{C_{Au-Si}}.$$

Here, C_{Al-G} and C_{Au-Si} are 9.09 x 10^{-7} F and 2.64 x 10^{-4} F as shown in a previous report.[1] The capacitance of graphene (C_G) is estimated as a function of the hole concentration (p) by $C_G = \frac{2q^2}{\hbar v_F \sqrt{\pi}} \sqrt{p}$ where q is elemental charge, $\hbar$ is the reduced plank constant, and v_F is Fermi velocity as 10^8 cm sec^{-1}. The reverse bias voltage dependent hole concentration (p) of graphene is extracted from the G peak shift of Raman spectra at 0 V and -5 V as shown in Figure S2 and can be expressed as a linear function of the reverse bias voltage by $p = 2.54 \times 10^{12} - 5.73 \times 10^{10} \cdot V$. The capacitance of silicon dioxide (C_{SiO2}) is calculated as $C_{SiO2} = \varepsilon_0 \varepsilon_{SiO2} \frac{A}{d}$, where ε_0 and ε_{SiO2} are vacuum permittivity and relative permittivity of silicon dioxide, A is 0.0144 cm^{-2} as the junction area, d is the thickness (4.2 Å) of silicon dioxide estimated by Schottky emission theory. The depletion capacitance (C_D) is calculated by $C_D = \varepsilon_0 \varepsilon_{Si} \frac{A}{W_D}$ where W_D is depletion width. The depletion width (W_D) is given by $W_D = \sqrt{\frac{2\varepsilon_0 \varepsilon_{Si}}{qN_A}(V_{Bi} - V_a - kT)\frac{1}{\eta}}$, where N_A and V_{Bi} are acceptor concentration and built-in potential extracted from Figure S1, V_a is applied voltage, k is Boltzmann constant, T is absolute temperature in Kelvin and η is the ideality factor. The capacitances of the interface state (C_{int}) and the inversion (C_{inv}) are expressed as Gaussian function. They are given by $C_{int} = P_{int} \cdot \exp^{-\left(\frac{V - V_{int}}{W_{int}}\right)^2} + C_O$, and $C_{inv} = P_{inv} \cdot \exp^{-\left(\frac{V - V_{inv}}{W_{inv}}\right)^2}$, where P_{int}, V_{int} and W_{int} are peak height, position and width of the interface state and where P_{inv}, V_{inv} and W_{inv} are peak height, position and width of the inversion, respectively. The linearly varied voltage-dependent capacitance (C_O) is attributed to the voltage dependent interface capacitance as shown in the previous study and which is expressed by $\alpha_{int} + \beta_{int} \cdot V$, where α_{int} and $\beta_{int} \cdot$ are constants. Table S1 shows fitting parameters for optical power dependent C-V experiment

data.[1]

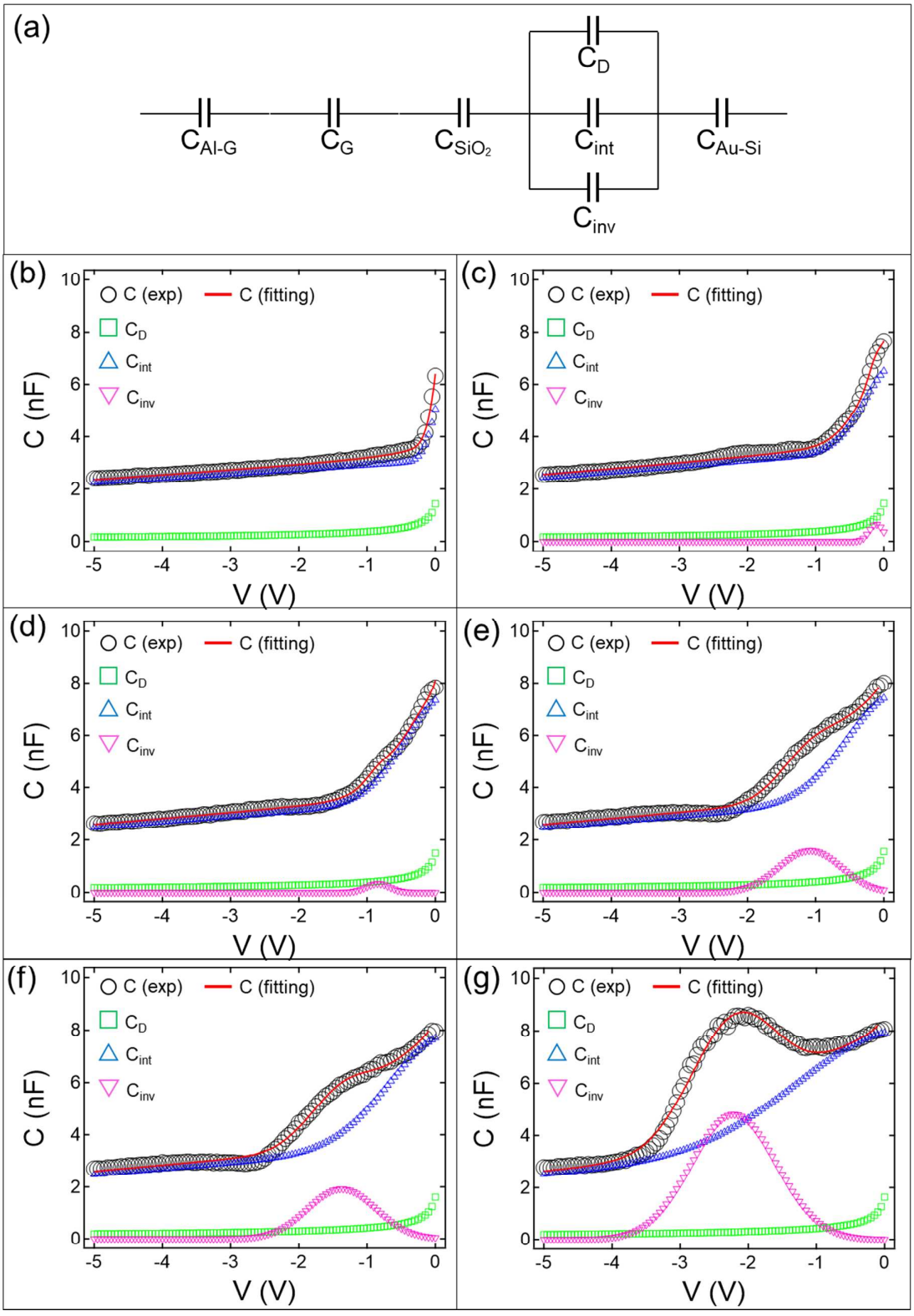
(a)
C_D
C_{Al-G}
C_G
C_{SiO_2}
C_{int}
C_{Au-Si}
C_{inv}
(b)
(c)
(d)
(e)
(f)
(g)
C (exp)
C (fitting)
C_D
C_{int}
C_{inv}
C (nF)
V (V)

Figure S3. (a) Equivalent circuit models for GOS Schottky diode. $C_{Al\text{-}G}$, C_G, C_{SiO2}, C_D, C_{int}, C_{inv}, C_{etc} and $C_{Au\text{-}Si}$ represent capacitances by aluminum-graphene, graphene, silicon dioxide, depletion region, interface state, inversion, rest and gold-silicon capacitance, respectively. (b)-(g) Experimental capacitances and fitted results based on the equivalent circuit model as a function of optical power at (b) dark state, (c) 14 $\mu W cm^{-2}$, (d) 71 $\mu W cm^{-2}$, (e) 142 $\mu W cm^{-2}$, (f) 0.7 $\mu W cm^{-2}$ and (g) 1.45 $\mu W cm^{-2}$.

Parameters	Value Optical power density ($\mu W\ cm^{-2}$)					
	Dark	14	71	142	712	1450
η	6.71	6.93	7.31	7.97	8.41	8.74
$C_{Al\text{-}G}$ (F)	9.09×10^{-7}	9.09×10^{-7}	9.09×10^{-7}	9.09×10^{-7}	9.09×10^{-7}	9.09×10^{-7}
$C_{Au\text{-}Si}$ (F)	2.64×10^{-4}	2.64×10^{-4}	2.64×10^{-4}	2.64×10^{-4}	2.64×10^{-4}	2.64×10^{-4}
C_{SiO2} (F)	1.18×10^{-7}	1.18×10^{-7}	1.18×10^{-7}	1.18×10^{-7}	1.18×10^{-7}	1.18×10^{-7}
P_{int} (F)	3.26×10^{-9}	3.26×10^{-9}	3.96×10^{-9}	3.98×10^{-9}	4.19×10^{-9}	4.27×10^{-9}
V_{int} (V)	0.186	0.186	0.186	0.186	0.186	0.186
W_{int} (V)	0.263	0.641	0.865	1.03	1.21	2.09
α_{int} (F)	3.09×10^{-9}	3.52×10^{-9}	3.56×10^{-9}	3.57×10^{-9}	3.61×10^{-9}	3.71×10^{-9}
β_{int} ($F\ V^{-1}$)	1.69×10^{-10}	2.14×10^{-10}	2.15×10^{-10}	2.19×10^{-10}	2.25×10^{-10}	2.40×10^{-10}
P_{inv} (F)	-	6.53×10^{-10}	3.38×10^{-10}	1.59×10^{-9}	1.92×10^{-9}	4.80×10^{-9}
V_{inv} (V)	-	0.112	0.842	1.08	1.37	2.21
W_{inv} (V)	-	0.145	0.243	0.638	0.698	0.882

Table S1. Summary of fitting parameters for the CV curves as shown in Figure S3.

4. REFERENCES

(1) Park, H. K.; Choi, J. Origin of Voltage-Dependent High Ideality Factors in Graphene–Silicon Diodes. Adv. Electron. Mater. 2018, 4, 1700317.

(2) Sze, S. M.; Ng, K. K. Physics of Semiconductor Devices, Third Edition; John Wiley & Sons, Inc., Hoboken, New Jersey, 2007; pp 136-139.

(3) Eckmann, A.; Felten, A.; Mishchenko, A.; Britnell, L.; Krupke, R.; Novoselov, K. S.; Casiraghi, C. Probing the Nature of Defects in Graphene by Raman Spectroscopy. *Nano Lett.* 2012, *12*, 3925–3930.

(4) Lazzeri, M.; Mauri, F. Nonadiabatic Kohn Anomaly in a Doped Graphene Monolayer. *Phys. Rev. Lett.* 2006, *97*, 29–32.

(5) Das, A.; Pisana, S.; Chakraborty, B.; Piscanec, S.; Saha, S. K.; Waghmare, U. V; Novoselov, K. S.; Krishnamurthy, H. R.; Geim, a K.; Ferrari, A. C.; Sood, A. K. Monitoring dopants by Raman scattering in an electrochemically top-gated graphene transistor *Nat. Nanotechnol.* 2008, *3*, 210–215.

(6) Deacon, R. S.; Chuang, K. C.; Nicholas, R. J.; Novoselov, K. S.; Geim, A. K. Cyclotron resonance study of the electron and hole velocity in graphene monolayers. *Phys. Rev. B - Condens. Matter Mater. Phys.* 2007, *76* (8), 2–5.